Fighting topological freezing in SU(N) Yang–Mills theories with the PTBC algorithm

Andrea Giorgieri

24/03/26

Lattice seminars @ BicQCD

In collaboration with:

C. Bonanno, J. L. Dasilva Golán, M. García Pérez, M. D'Elia

Based on:

Eur. Phys. J. C 84 (2024) 916 [arXiv:2403.13607]

Phys. Rev. D XX (forthcoming) [arXiv:2511.07355]

Outline

1. **Introduction:** topological charge in lattice SU(N) Yang–Mills theories
2. **Main topic:** topological freezing and the PTBC algorithm
3. **1st application:** topological effects in the SU(3) TGF coupling
4. **2nd application:** topological effects in the SU(N) gradient-flow scales
5. **Future application:** the PTBC algorithm with multicanonical method
6. **Conclusions:** summary of results and future outlooks

Finite-action gauge configurations in QCD and QCD-like theories in the continuum are classified by the integer-valued topological charge:

$$Q = \int d^4x \frac{g^2}{32\pi^2} \epsilon_{\mu\nu\rho\sigma} \mathrm{Tr}\left[F_{\mu\nu} F_{\rho\sigma}\right] \in \mathbb{Z}$$

We cannot probe the *topological sector* of the Universe, but the *density* of Q and the existence of *localized structures* with non-trivial Q (instantons, sphalerons) have phenomenological implications:

η' mass
θ-dependence
strong CP problem
axion mass and abundance

Reproducing topological features in lattice simulations with controlled *finite-volume effects* requires to explore the different topological sectors

4D SU(N) Yang–Mills: the pure-gauge theory with N colors shares topological (and others) features with full QCD, also theoretically interesting for large-N limit and testbed for algorithmic advancements

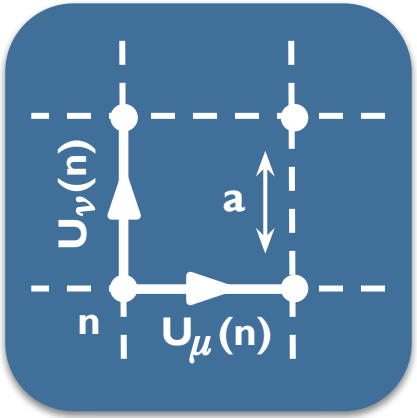

Wilson action: the continuum Euclidean action

$$S = \int d^4x \frac{1}{2}\mathrm{Tr}\left[F_{\mu\nu}F_{\mu\nu}\right] , \quad F_{\mu\nu} = \partial_\mu A_\nu - \partial_\nu A_\mu + ig\left[A_\mu, A_\nu\right]$$

is discretized as

$$S = -\frac{\beta}{2N}\sum_{n,\mu\neq\nu}\mathrm{ReTr}\left[P_{\mu\nu}(n)\right] , \quad \beta = 2N/g^2$$

and a generic observable is given by

$$\langle\mathcal{O}\rangle = \frac{1}{Z}\int\prod_{n,\mu} dU_\mu(n) e^{-S[U]}\mathcal{O}[U] , \quad Z = \int\prod_{n,\mu} dU_\mu(n) e^{-S[U]}$$

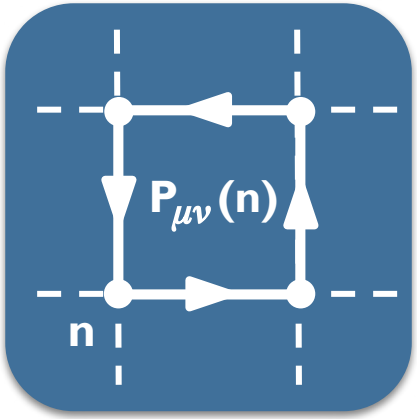

Introduction – Gradient flow

Regularization with *gradient flow* (Lüscher, 2010):
gauge links $U_\mu(n)$ evolved in a flow-time with

$$\partial_t V_\mu(n,t) = -g^2 \left[\partial_{n,\mu} S(V)\right] V_\mu(n,t)\,, \quad V_\mu(n,t=0) = U_\mu(n)$$

→ Fields smoothed in a radius $\sqrt{8t}$
(notice $[t] = [\text{length}]^2$)

Gauge observables evaluated at $t > 0$ are renormalized:
they remain finite in the continuum limit $a \to 0$.

Introduction – Gradient flow

Regularization with *gradient flow* (Lüscher, 2010):
gauge links $U_\mu(n)$ evolved in a flow-time with

$$\partial_t V_\mu(n,t) = -g^2 \left[\partial_{n,\mu} S(V)\right] V_\mu(n,t)\,, \quad V_\mu(n,t=0) = U_\mu(n)$$

→ Fields smoothed in a radius $\sqrt{8t}$ (notice $[t] = [\text{length}]^2$)

Gauge observables evaluated at $t > 0$ are renormalized:
they remain finite in the continuum limit $a \to 0$.

The flowed energy density $E(t) \geq 0$ can be used to define a renormalized 't Hooft coupling:

$$\lambda(\mu) = N g^2(\mu) = \mathcal{N} \langle t^2 E(t) \rangle \big|_{\sqrt{8t}=\mu^{-1}} = \lambda_{\overline{MS}}(\mu) + O(\lambda^2_{\overline{MS}})$$

The renormalization scale runs with the inverse of t .

On the lattice, clover discretization of the energy:

$$E_{\text{clov}}(t) = \frac{1}{2V} \sum_n \text{Tr}\left[C_{\mu\nu}(n,t) C_{\mu\nu}(n,t)\right]$$

$C_{\mu\nu}(n)$ ~

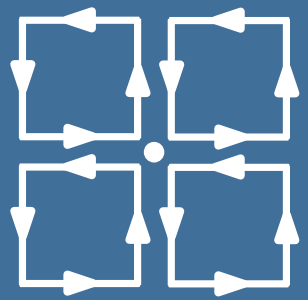

Introduction – Topological charge on the lattice

Continuum: Configurations with different Q cannot be deformed into one another by continuous transformations, topological sectors separated by *infinite-energy barriers* and

$$S \geq \frac{8\pi^2}{g^2}|Q|$$

Introduction – Topological charge on the lattice

Continuum: Configurations with different Q cannot be deformed into one another by continuous transformations, topological sectors separated by *infinite-energy barriers* and

$$S \geq \frac{8\pi^2}{g^2}|Q|$$

Lattice: Topology not well-defined at finite lattice spacing.
Non-integer discretization with gradient flow:

$$Q_{\text{clov}}(t) = \frac{1}{32\pi^2}\epsilon_{\mu\nu\rho\sigma}\sum_n \text{Tr}\left[C_{\mu\nu}(n,t)C_{\rho\sigma}(n,t)\right]$$

Near-integer plateau reached after some flow:

$$Q = \text{round}\left[Q_{\text{clov}}(t_Q)\right]$$

Choice of t_Q requires more care at coarse spacings or high-temperatures:
too much flow can destroy instantons

$N = 3,\ \beta = 6.765,\ V = 30^2 46^2$

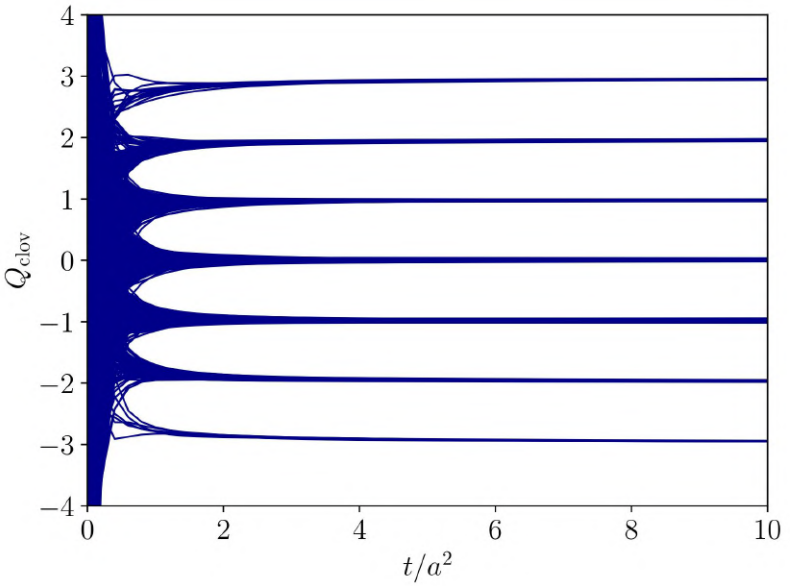

Main topic – Topological freezing

In an MCMC simulation an algorithm generates a stochastic sequence of correlated field configurations $\{U_1, U_2, \ldots, U_{N_s}\}$ such that

$$\bar{\mathcal{O}} = \frac{1}{N_s} \sum_k \mathcal{O}[U_k] \qquad \delta\bar{\mathcal{O}} = \sqrt{\frac{2\tau_{\mathcal{O}}}{N_s}} \sigma_{\mathcal{O}}$$

Integrated autocorrelation time $\tau_{\mathcal{O}}$*:*

- Represents separation between effectively independent samples
- Depends on the observable and the algorithm
- Precise results require $N_s \gg \tau_{\mathcal{O}}$

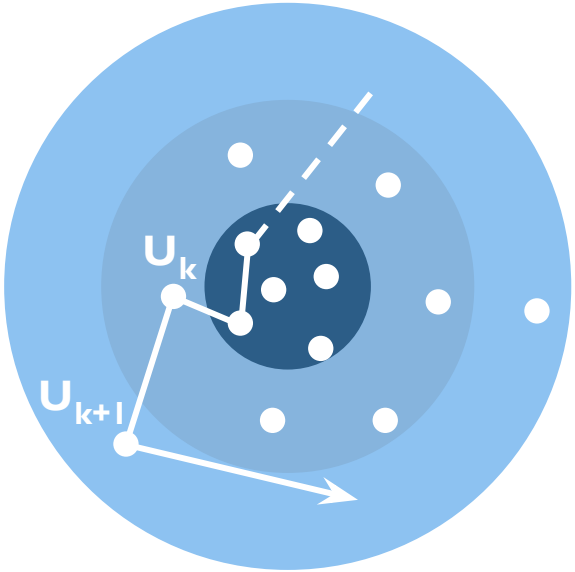

Main topic – Topological freezing

As $a \to 0$, high-energy barriers develop between topological sectors.
Markov chain frozen in fixed sector, usually $Q = 0$, for long time: $\tau_Q \to \infty$

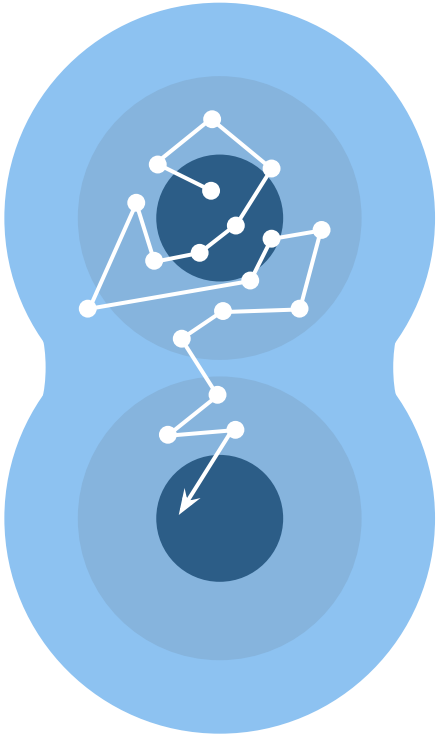

Main topic – Topological freezing

As $a \to 0$, high-energy barriers develop between topological sectors.
Markov chain frozen in fixed sector, usually $Q = 0$, for long time: $\tau_Q \to \infty$

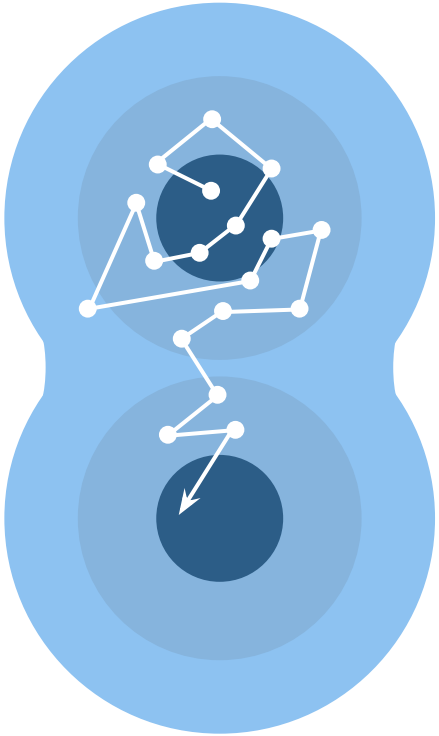

Effect: prevents determination of topological observables like the susceptibility $\chi = \langle Q^2 \rangle / V$, but also increases $\tau_{\mathcal{O}}$ for every observable correlated with Q:

$$\langle \mathcal{O} \rangle = \sum_{Q \in \mathbb{Z}} P_Q \langle \mathcal{O} \rangle_Q \,, \quad \sum_{Q \in \mathbb{Z}} P_Q = 1 \,.$$

Relevant for the flowed energy density:

$$S \geq \frac{8\pi^2}{g^2} |Q| \Rightarrow \langle E(t \gg 1) \rangle_Q \propto |Q|$$

Main topic – Topological freezing

As $a \to 0$, high-energy barriers develop between topological sectors.
Markov chain frozen in fixed sector, usually $Q = 0$, for long time: $\tau_Q \to \infty$

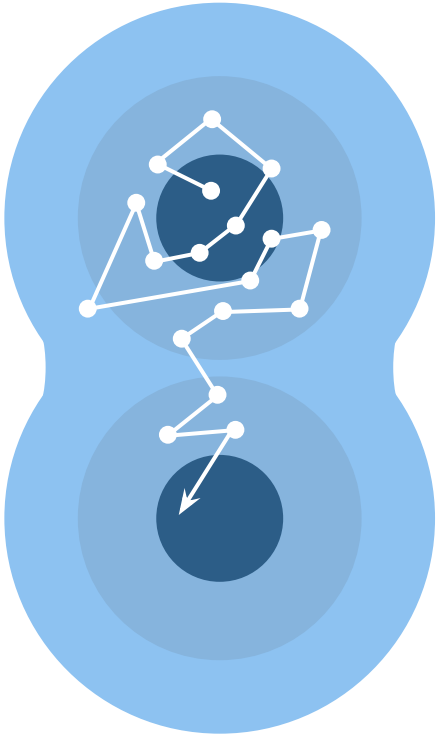

Effect: prevents determination of topological observables like the susceptibility $\chi = \langle Q^2 \rangle / V$, but also increases $\tau_{\mathcal{O}}$ for every observable correlated with Q:

$$\langle \mathcal{O} \rangle = \sum_{Q \in \mathbb{Z}} P_Q \langle \mathcal{O} \rangle_Q \,, \quad \sum_{Q \in \mathbb{Z}} P_Q = 1 \,.$$

Relevant for the flowed energy density:

$$S \geq \frac{8\pi^2}{g^2} |Q| \Rightarrow \langle E(t \gg 1) \rangle_Q \propto |Q|$$

Workaround: determination of $\langle \mathcal{O} \rangle_0 = \langle \mathcal{O} \delta_{Q,0} \rangle / \langle \delta_{Q,0} \rangle$ using only $Q = 0$ configurations (*projection* into $Q = 0$)
This is known to introduce biases vanishing only at infinite volume, mitigating freezing at the algorithmic level is better

Main topic – PTBC algorithm: general idea

Parallel Tempering (PT): simulate multiple replicas $r = 0, 1, \ldots, N_r - 1$ of the lattice in parallel, differing only for a parameter $c(r)$ which interpolates between the physical value $c(0)$ and one for which there is no freezing $c(N_r - 1)$

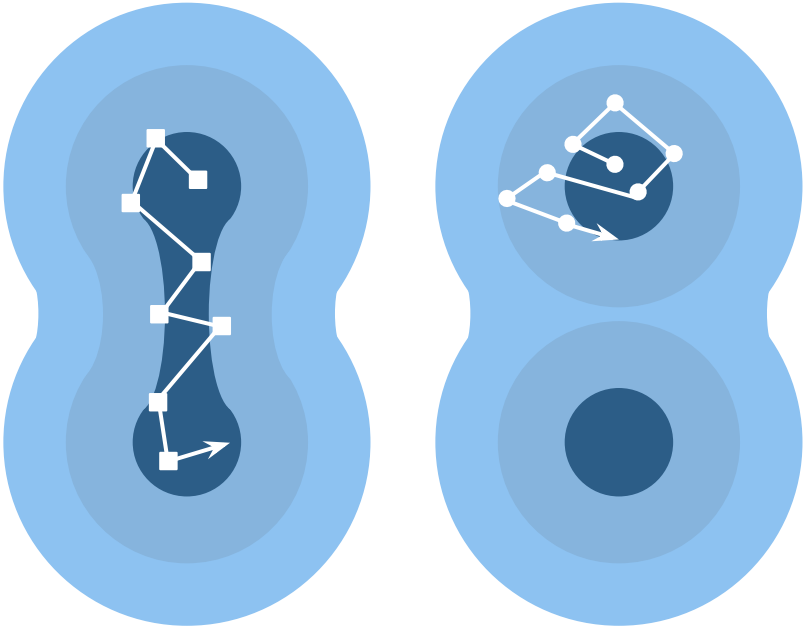

Main topic – PTBC algorithm: general idea

Parallel Tempering (PT): simulate multiple replicas $r = 0, 1, \ldots, N_r - 1$ of the lattice in parallel, differing only for a parameter $c(r)$ which interpolates between the physical value $c(0)$ and one for which there is no freezing $c(N_r - 1)$

Replicas are updated independently with a standard algorithm.

Every few steps, swaps between adjacent field configurations $(r, s = r + 1)$ are proposed and accepted with probability (Metropolis algorithm)

$$p(r, s) = \min\{1, e^{-\Delta S_{\text{swap}}}\}$$

This ensures the correct distribution on the physical replica, on which measures are taken.

Decorrelation transferred from the unphysical to the physical replica thanks to swaps.

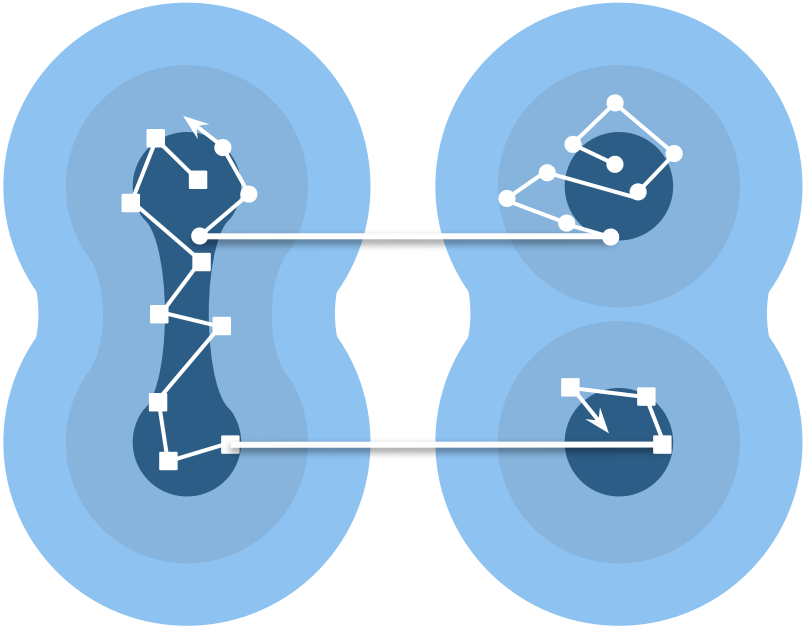

Main topic – PTBC algorithm: implementation

Open Boundary Conditions (OBCs) remove barriers between topological sectors, but Periodic Boundary Conditions (PBCs) have smaller finite-volume corrections

Main topic – PTBC algorithm: implementation

Open Boundary Conditions (OBCs) remove barriers between topological sectors, but Periodic Boundary Conditions (PBCs) have smaller finite-volume corrections

PT on Boundary Conditions (PTBC) (Hasenbusch, 2017; Bonanno et al., 2021; Bonanno et al., 2024):

Replicas differ for boundary conditions on small 3d sub-lattice, the *defect* D

Links crossing D multiplied by $c(r)$

Periodic: $c(0) = 1$ Open: $c(N_r - 1) = 0$ Others: $0 < c(r) < 1$

Simple implementation: $S_r[U_r] = -\frac{\beta}{2N} \sum_{n,\mu\neq\nu} K^{(r)}_{\mu\nu}(n) \mathrm{ReTr}\left[P^{(r)}_{\mu\nu}(n)\right]$

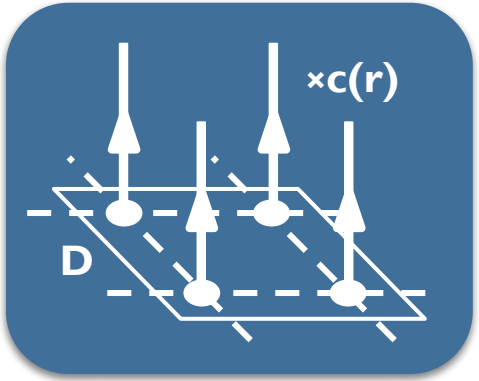

Main topic – PTBC algorithm: implementation

Open Boundary Conditions (OBCs) remove barriers between topological sectors, but Periodic Boundary Conditions (PBCs) have smaller finite-volume corrections

PT on Boundary Conditions (PTBC) (Hasenbusch, 2017; Bonanno et al., 2021; Bonanno et al., 2024):

Replicas differ for boundary conditions on small 3d sub-lattice, the *defect* D

Links crossing D multiplied by $c(r)$

Periodic: $c(0) = 1$ Open: $c(N_r - 1) = 0$ Others: $0 < c(r) < 1$

Simple implementation: $S_r[U_r] = -\frac{\beta}{2N} \sum_{n,\mu\neq\nu} K^{(r)}_{\mu\nu}(n) \mathrm{ReTr}\left[P^{(r)}_{\mu\nu}(n)\right]$

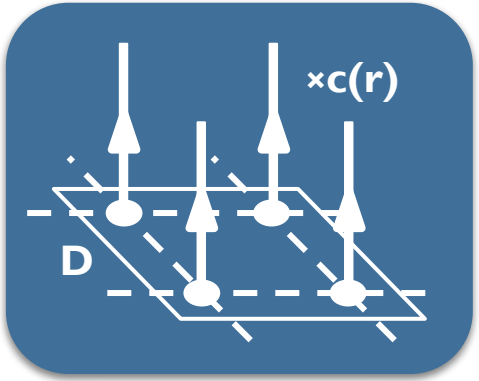

- $K^{(r)}_{\mu\nu}(n) \neq 1$ only on D: computation of ΔS_{swap} is cheap
- Generalizes simply to full QCD (already used in Bonanno et al., 2024)
- Measures on replica with PBCs: benefits of OBCs without their drawbacks

Main topic – PTBC algorithm: optimizations

The defect is the source of topological fluctuations, so to improve performances:

- D on the physical replica is translated randomly during the simulation (action unchanged, no Metropolis step needed)
- Local updates are more frequent around D
- Size of D $\ell_d \sim 0.18 - 0.20 \text{ fm}$ kept constant in physical units

Main topic – PTBC algorithm: optimizations

The defect is the source of topological fluctuations, so to improve performances:

- D on the physical replica is translated randomly during the simulation (action unchanged, no Metropolis step needed)
- Local updates are more frequent around D
- Size of D $\ell_d \sim 0.18 - 0.20$ fm kept constant in physical units

Configurations should move between replicas in a sort of random walk:

- N_r and $c(r)$ dynamically tuned in short simulations to achieve constant swap acceptance $a(r, r+1) \simeq 20\%$

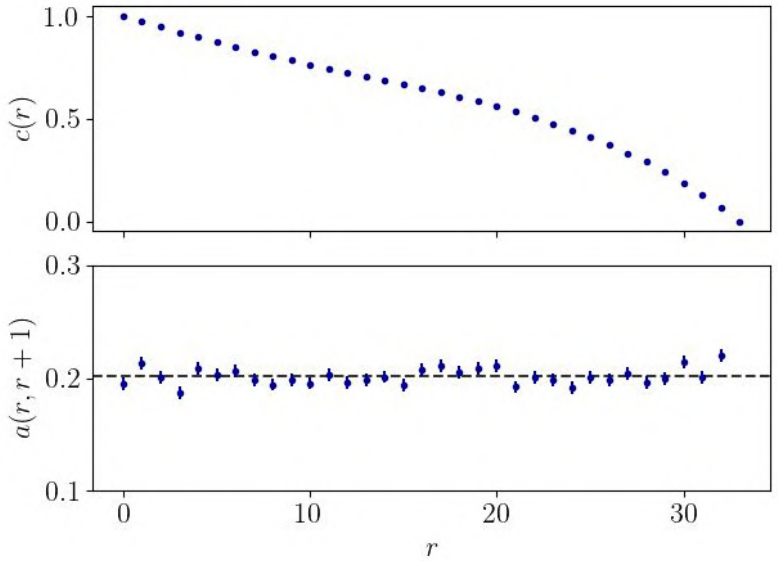

$N = 3,\ \beta = 6.765,\ V = 30^2 46^2$

$N_r = 34,\ V_d = 6^3$

Main topic – PTBC algorithm: effectiveness

MC histories of Q with PTBC and standard algorithm (heat-bath + 12 over-relaxation sweeps)
With PTBC, lattice sweeps counted on all replicas to account for extra computational effort

Standard algorithm frozen even with coarsest SU(5) lattice spacing in these works

Integrated autocorrelation time τ_{Q^2} of Q^2 for quantitative comparison:

	PTBC	Standard
Q^2	$0.084(2)$	$0.08(2)$
τ_{Q^2}	$2.5(3) \cdot 10^2$	$> 10^5$

Gain of PTBC gets larger in the continuum limit

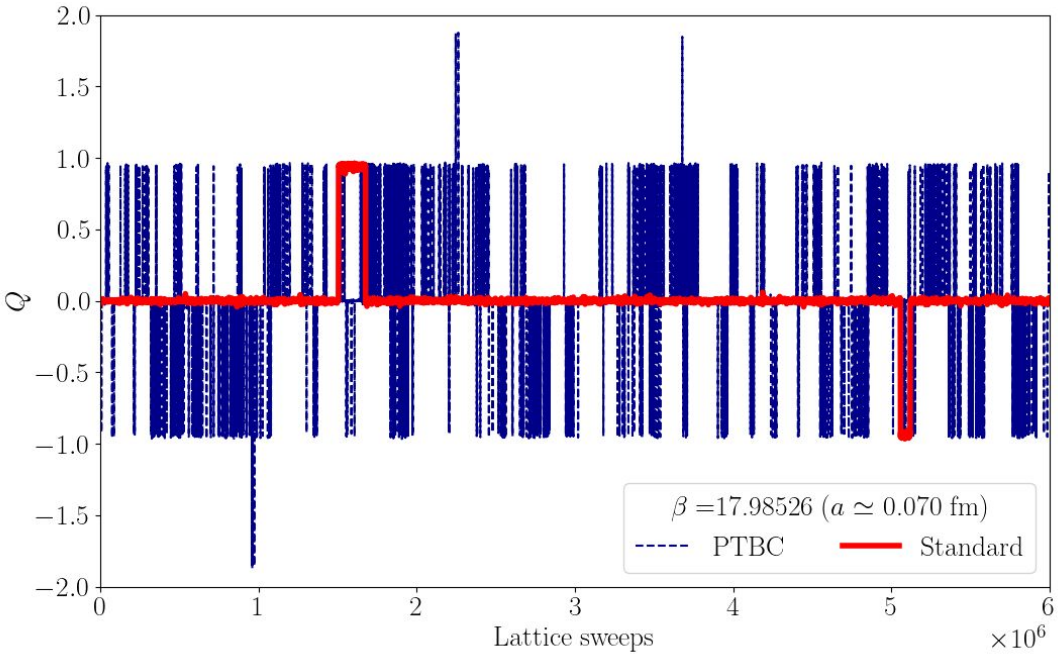

Main topic – PTBC algorithm: effectiveness

Scaling of required N_r and τ_{Q^2} (Bonanno, 2025):

At fixed 20% acceptance, required replicas:

$$N_r \simeq CNL_d^{3/2} = CN(\ell_d/a)^{3/2}\,,\ C = 0.80(5)$$

Autocorrelation of periodic replica:

$$\tau_0(Q^2) \simeq C'(\ell_d\sqrt{\sigma})^{-2}(a\sqrt{\sigma})^{-2}N^{0.5}$$

$$C' = 0.081(5)$$

Effective autocorrelation $\tau(Q^2) = N_r\tau_0(Q^2)$:

$$\tau(Q^2) \simeq 0.065(\ell_d\sqrt{\sigma})^{-0.5}(a\sqrt{\sigma})^{-3.5}N^{1.5}$$

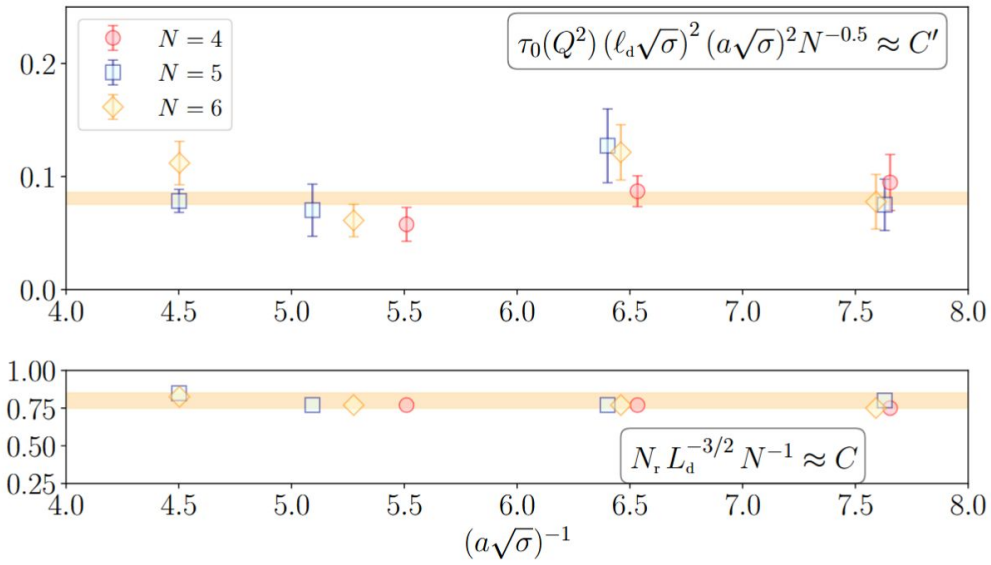

Main topic – PTBC algorithm: effectiveness

Scaling of required N_r and τ_{Q^2} (Bonanno, 2025):

At fixed 20% acceptance, required replicas:

$$N_r \simeq CNL_d^{3/2} = CN(\ell_d/a)^{3/2}\,,\ \ C = 0.80(5)$$

Autocorrelation of periodic replica:

$$\tau_0(Q^2) \simeq C'(\ell_d\sqrt{\sigma})^{-2}(a\sqrt{\sigma})^{-2}N^{0.5}$$

$$C' = 0.081(5)$$

Effective autocorrelation $\tau(Q^2) = N_r\tau_0(Q^2)$:

$$\tau(Q^2) \simeq 0.065(\ell_d\sqrt{\sigma})^{-0.5}(a\sqrt{\sigma})^{-3.5}N^{1.5}$$

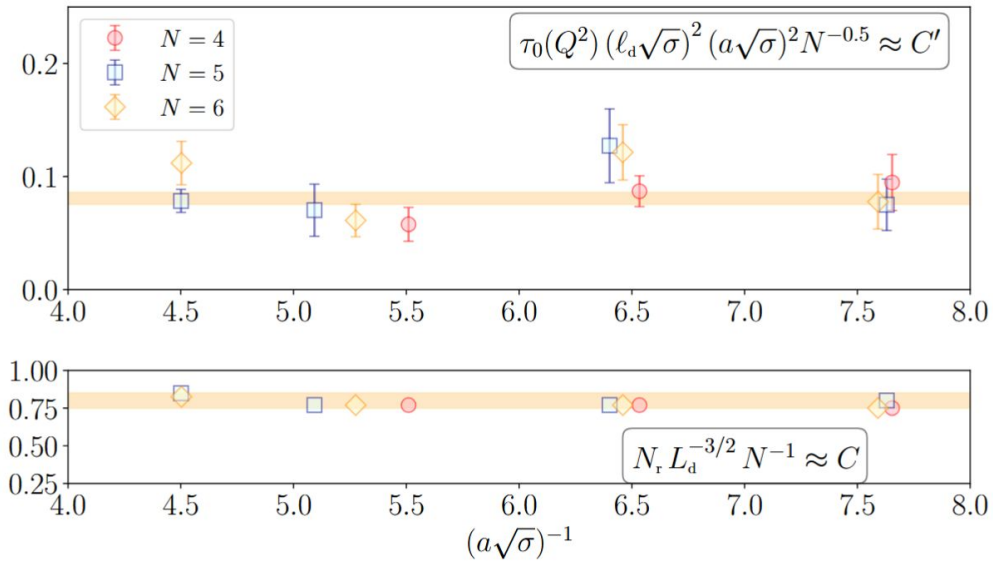

Mild improvement increasing defect size, but if too large the overhead of swaps becomes relevant and N_r can be limited by available memory

Scaling of τ_{Q^2} in a and N is polynomial instead of exponential (Del Debbio et al, 2002; Bonanno et al, 2018)

1st application – SU(3) TGF coupling: motivation

End goal: Λ-parameter, RG-invariant scheme-dependent energy scale

$$\Lambda_s = \mu[b_0\lambda_s(\mu)]^{-\frac{b_1}{2b_0^2}} e^{-\frac{1}{2b_0\lambda_s(\mu)}} \exp\left\{-\int_0^{\lambda_s(\mu)} dx \left(\frac{1}{2\beta_s(x)} + \frac{1}{2b_0^2x^2} - \frac{b_1}{2b_0^2x}\right)\right\}$$

Step-scaling method: flow $\lambda_s(\mu)$ in steps $\mu \longrightarrow \mu/2$ from $\mu_{\rm pt} = 2^n\mu_{\rm had}$ to $\mu_{\rm had}$ and determine

$$\frac{\Lambda_s}{\mu_{\rm had}} = \frac{\mu_{\rm pt}}{\mu_{\rm had}}\frac{\Lambda_s}{\mu_{\rm pt}} = 2^n \left.\frac{\Lambda_s}{\mu_{\rm pt}}\right|_{\rm pt}$$

1st application – SU(3) TGF coupling: motivation

End goal: Λ-parameter, RG-invariant scheme-dependent energy scale

$$\Lambda_s = \mu[b_0\lambda_s(\mu)]^{-\frac{b_1}{2b_0^2}} e^{-\frac{1}{2b_0\lambda_s(\mu)}} \exp\left\{-\int_0^{\lambda_s(\mu)} dx \left(\frac{1}{2\beta_s(x)} + \frac{1}{2b_0^2x^2} - \frac{b_1}{2b_0^2x}\right)\right\}$$

Step-scaling method: flow $\lambda_s(\mu)$ in steps $\mu \longrightarrow \mu/2$ from $\mu_{\rm pt} = 2^n\mu_{\rm had}$ to $\mu_{\rm had}$ and determine

$$\frac{\Lambda_s}{\mu_{\rm had}} = \frac{\mu_{\rm pt}}{\mu_{\rm had}}\frac{\Lambda_s}{\mu_{\rm pt}} = 2^n \left.\frac{\Lambda_s}{\mu_{\rm pt}}\right|_{\rm pt}$$

Twofold objective: 1) With SU(3) Twisted Gradient Flow (TGF) scheme, check if $Q = 0$ coupling $\lambda^{(0)}_{TGF}$ gives the same result as λ_{TGF} , measurable only with PTBC due to freezing

2) Check if a frozen standard algorithm and PTBC agree on $\lambda^{(0)}_{TGF}$: with freezing, not obvious that fluctuations of the *density* of Q in $Q = 0$ sector are correctly sampled and the lack of *ergodicity* is bypassed

1st application – SU(3) TGF coupling: scheme definition

Geometry: SU(N) theory discretized on lattice of size $L^2 \times L_s^2$ with $L_s = L/N$ for directions 1, 2

On the plane (1,2), Twisted Boundary Conditions (TBCs) (Arroyo and Okawa, 1983): same as Periodic BCs up to a phase factor implemented similarly to the PTBC defect

$$S[U] = -\frac{\beta}{2N} \sum_{n,\mu\neq\nu} Z^*_{\mu\nu}(n) \mathrm{ReTr}\left[P_{\mu\nu}(n)\right]$$

TBCs motivated by *twisted volume reduction* (Arroyo and Okawa, 2010): up to $O(1/N^2)$ corrections, dynamics should equivalent to one with effective volume $V_{\mathrm{eff}} = N^2 V = L^4$ and PBCs

1st application – SU(3) TGF coupling: scheme definition

Geometry: SU(N) theory discretized on lattice of size $L^2 \times L_s^2$ with $L_s = L/N$ for directions 1, 2

On the plane (1,2), Twisted Boundary Conditions (TBCs) (Arroyo and Okawa, 1983): same as Periodic BCs up to a phase factor implemented similarly to the PTBC defect

$$S[U] = -\frac{\beta}{2N} \sum_{n,\mu\neq\nu} Z^*_{\mu\nu}(n) \mathrm{ReTr}\left[P_{\mu\nu}(n)\right]$$

TBCs motivated by *twisted volume reduction* (Arroyo and Okawa, 2010): up to $O(1/N^2)$ corrections, dynamics should equivalent to one with effective volume $V_{\text{eff}} = N^2 V = L^4$ and PBCs

Coupling: Finite-volume $l = aL$ renormalization scheme:

$$\mu = 1/(cl) \quad (c = 0.3)$$

Coupling defined with flowed energy density:

$$\lambda_{TGF}(\mu) = \mathcal{N}(c) \left\langle t^2 E(t) \right\rangle \Big|_{\sqrt{8t}=\mu^{-1}} \qquad \lambda^{(0)}_{TGF}(\mu) = \mathcal{N}(c) \left. \frac{\langle t^2 E(t) \delta_{Q,0} \rangle}{\langle \delta_{Q,0} \rangle} \right|_{\sqrt{8t}=\mu^{-1}}$$

1st application – SU(3) TGF coupling: step scaling

Step A: Tune β with $L = 12, 18, 24$ to get target $u_{\rm tg} \equiv \lambda_{\rm TGF}(\mu)$
$\mu \propto 1/aL$: same physical volume and different lattice spacing,
defines Line of Constant Physics $\rm LCP1$

Step B: Same β with $L \longrightarrow 2L$ gives $\lambda_{\rm TGF}(\mu/2)$ up to lattice artifacts,
$a \to 0$ limit to get the *step-scaling function* $\sigma_{\rm tg} = \sigma(u_{\rm tg})$

Step C: Tune β with $2L$ to get $\sigma_{\rm tg} = \lambda_{\rm TGF}(\mu/2)$ compensating artifacts.
This defines $\rm LCP2$ with $\mu \to \mu/2$

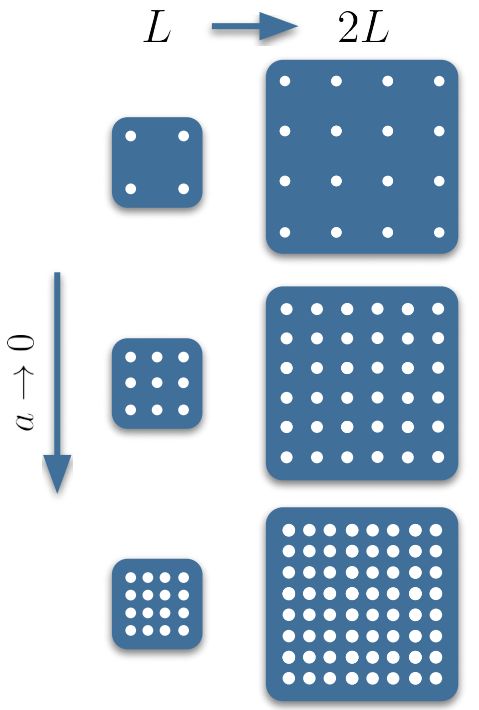

$u = \lambda(\mu) \quad \sigma(u) = \lambda(\mu/2)$

1st application – SU(3) TGF coupling: step scaling

Step A: Tune β with $L = 12, 18, 24$ to get target $u_{\rm tg} \equiv \lambda_{\rm TGF}(\mu)$
$\mu \propto 1/aL$: same physical volume and different lattice spacing,
defines Line of Constant Physics $\rm LCP1$

Step B: Same β with $L \longrightarrow 2L$ gives $\lambda_{\rm TGF}(\mu/2)$ up to lattice artifacts,
$a \to 0$ limit to get the *step-scaling function* $\sigma_{\rm tg} = \sigma(u_{\rm tg})$

Step C: Tune β with $2L$ to get $\sigma_{\rm tg} = \lambda_{\rm TGF}(\mu/2)$ compensating artifacts.
This defines $\rm LCP2$ with $\mu \to \mu/2$

Check 1: The step $\mu \to \mu/2$ should not depend on chosen coupling, so
$\lambda_{\rm TGF}$ should be constant on LCPs tuned with $\lambda^{(0)}_{\rm TGF}$

Check 2: If topological freezing does not bias $\lambda^{(0)}_{\rm TGF}$, its values measured
with a frozen algorithm and PTBC should agree

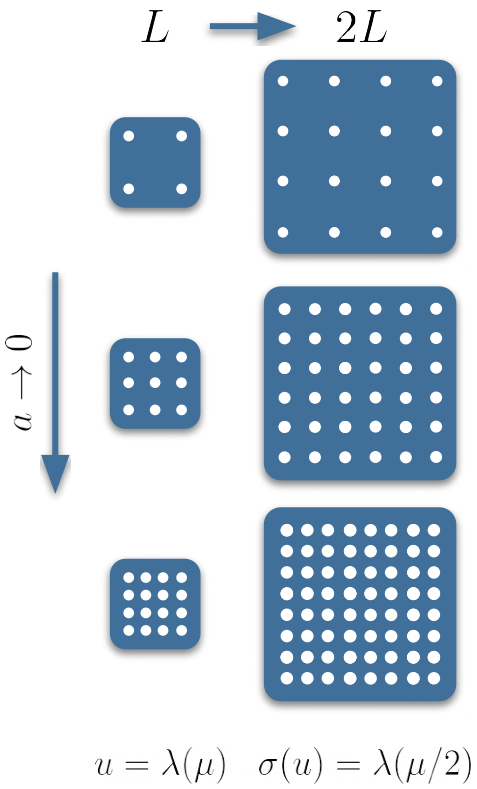

1st application – SU(3) TGF coupling: results (arXiv:2403.13607)

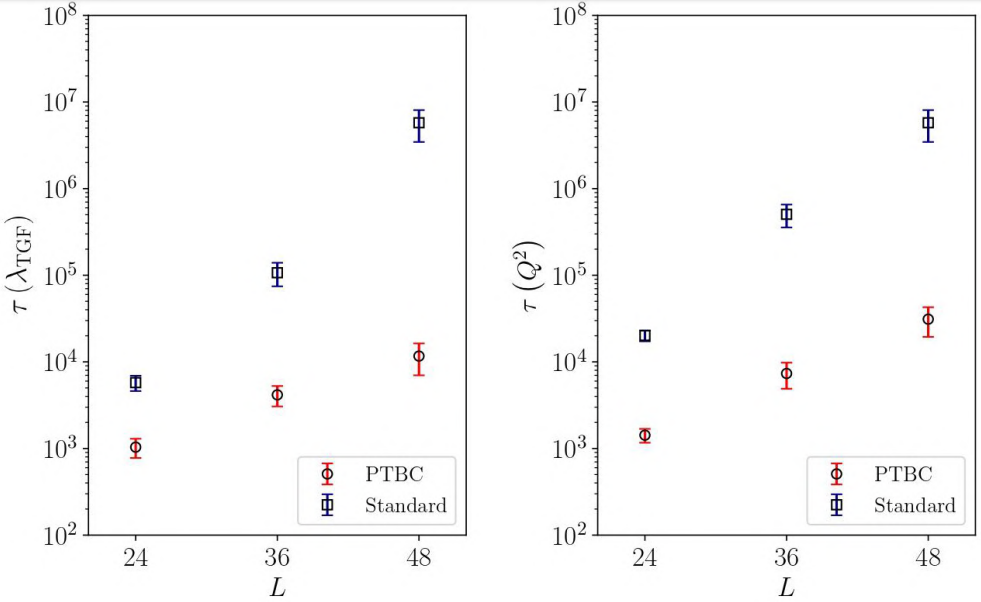

PTBC performance:

Large reduction of $\tau(Q^2)$ and $\tau(\lambda_{\mathrm{TGF}})$, Q sampled reliably and no need to use $\lambda^{(0)}_{\mathrm{TGF}}$. Benefit to statistical precision also because $Q \neq 0$ confs are not discarded.

1st application – SU(3) TGF coupling: results (arXiv:2403.13607)

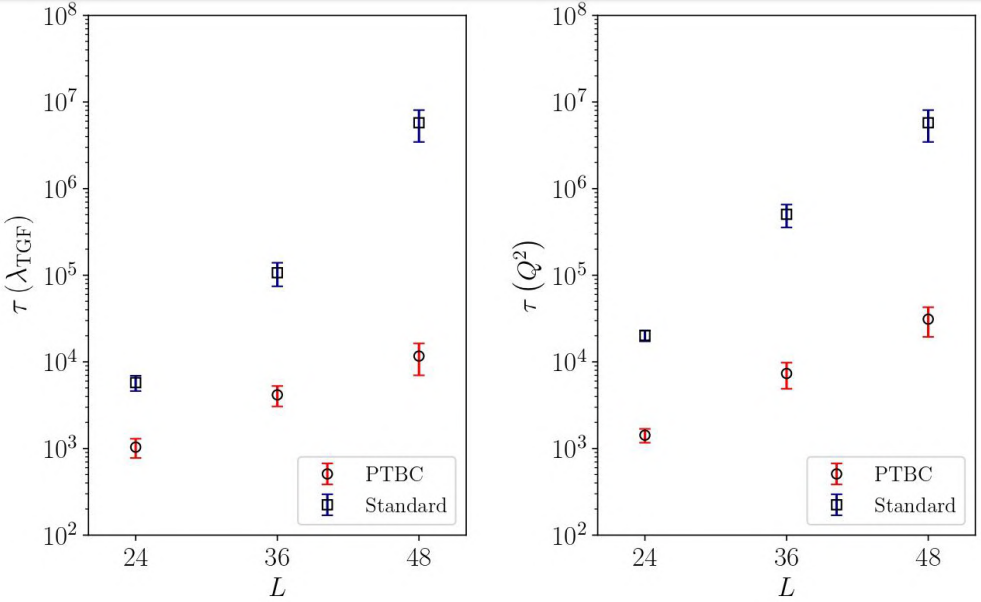

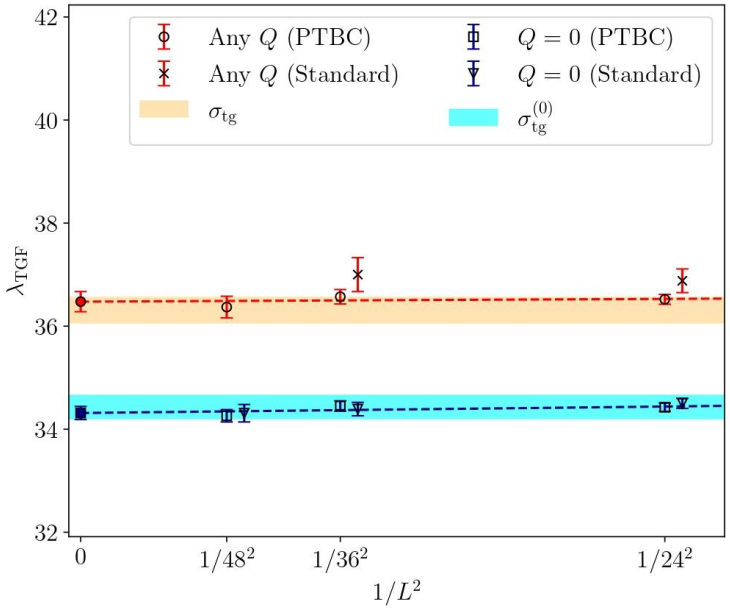

PTBC performance:
Large reduction of $\tau(Q^2)$ and $\tau(\lambda_{\rm TGF})$, Q sampled reliably and no need to use $\lambda^{(0)}_{\rm TGF}$. Benefit to statistical precision also because $Q \neq 0$ confs are not discarded.

Step-scaling:
same $\lambda^{(0)}_{\rm TGF}$ with frozen algorithm and PTBC, $\lambda_{\rm TGF}$ is constant on LCPs tuned with $\lambda^{(0)}_{\rm TGF}$, so no bias from severe topological freezing.

1st application – SU(3) TGF coupling: results (arXiv:2403.13607)

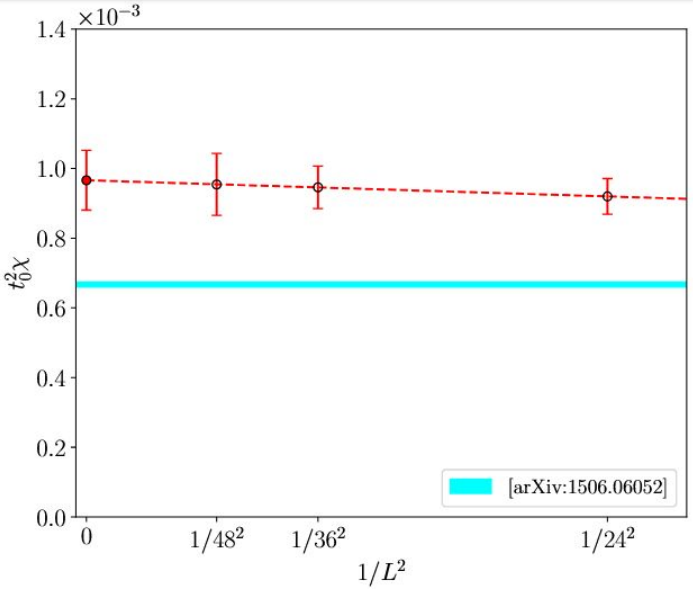

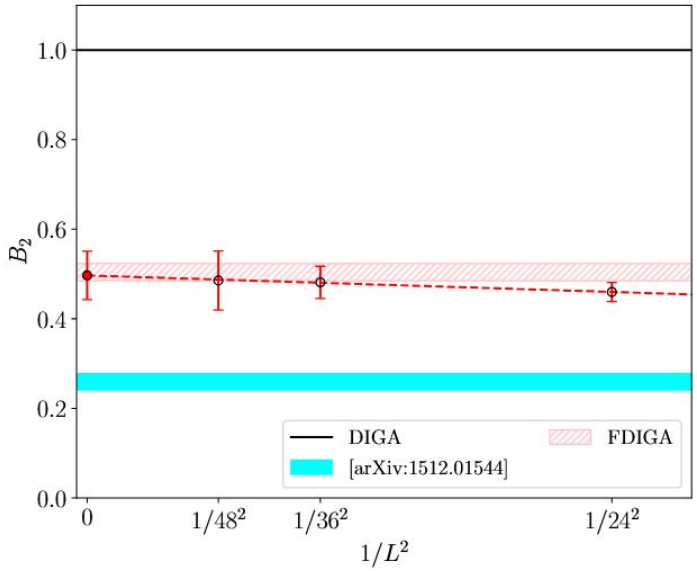

PTBC allows to determine χ and $B_2 = \left[\langle Q^4\rangle - 3\langle Q^2\rangle^2\right]/\langle Q^2\rangle$. Physical volumes are small, but:

- Small artifacts are a further check that $\lambda^{(0)}_{\mathrm{TGF}}$ can be used to tune LCPs
- Agreement with *Fractional Dilute Instanton Gas Approximation* (FDIGA) (Arroyo, 2023 for a review) using measured $\langle Q^2\rangle$ to determine B_2 by consistency relation

2nd application – SU(N) gradient-flow scales: motivation

End goal: From step-scaling, $\Lambda_{\mathrm{TGF}}/\mu_{\mathrm{had}}$ for $N = 3, 5, 8$. Set the *gradient flow scales* t_0, t_1, w_0^2 and

$$\mu_{\mathrm{had}}\sqrt{8t_0} \quad \Longrightarrow \quad \Lambda_{\mathrm{TGF}}\sqrt{8t_0} = \Lambda_{\mathrm{TGF}}/\mu_{\mathrm{had}} \cdot \mu_{\mathrm{had}}\sqrt{8t_0}$$

2nd application – SU(N) gradient-flow scales: motivation

End goal: From step-scaling, $\Lambda_{\rm TGF}/\mu_{\rm had}$ for $N = 3, 5, 8$. Set the *gradient flow scales* t_0, t_1, w_0^2 and

$$\mu_{\rm had}\sqrt{8t_0} \quad \Longrightarrow \quad \Lambda_{\rm TGF}\sqrt{8t_0} = \Lambda_{\rm TGF}/\mu_{\rm had} \cdot \mu_{\rm had}\sqrt{8t_0}$$

Gradient-flow scales are defined from flowed energy density $E(t)$, correlated with Q
Expected finite-volume effects:

$$t_0(\text{Any } Q) : \sim e^{-ML}$$
$$t_0^{(0)}(Q = 0) : \sim e^{-ML} + 1/V \quad \text{(Brower et al., 2003)}$$

Secondary goals: 1) Employ PTBC to quantify and avoid finite-volume effects on scales due to $Q = 0$ projection

2) Check $1/N^2$ suppression of finite-volume effects expected from *twisted volume reduction* using *Twisted Boundary Conditions* (TBCs) (Arroyo and Okawa, 1983)

2nd application – SU(N) gradient-flow scales: definitions

Scale t_0 defined for SU(3) as

$$\langle t^2 E(t)\rangle\big|_{t=t_0} = 0.3 \implies \sqrt{8t_0} \simeq 0.5 \text{ fm}$$

Extended to SU(N) as

$$\varphi(t_0) = \frac{9}{80} = 0.1125\,, \quad \varphi(t) \equiv \frac{N}{N^2-1}\langle t^2 E(t)\rangle$$

Other scales:

$$\varphi(t_1) = \frac{9}{160} = 0.05625\,, \quad t\,\frac{d\varphi(t)}{dt}\bigg|_{t=w_0^2} = \frac{9}{80} = 0.1125$$

Projection to $Q = 0$:

$$\langle E(t)\rangle \longrightarrow \langle E(t)\delta_{Q,0}\rangle / \langle \delta_{Q,0}\rangle$$

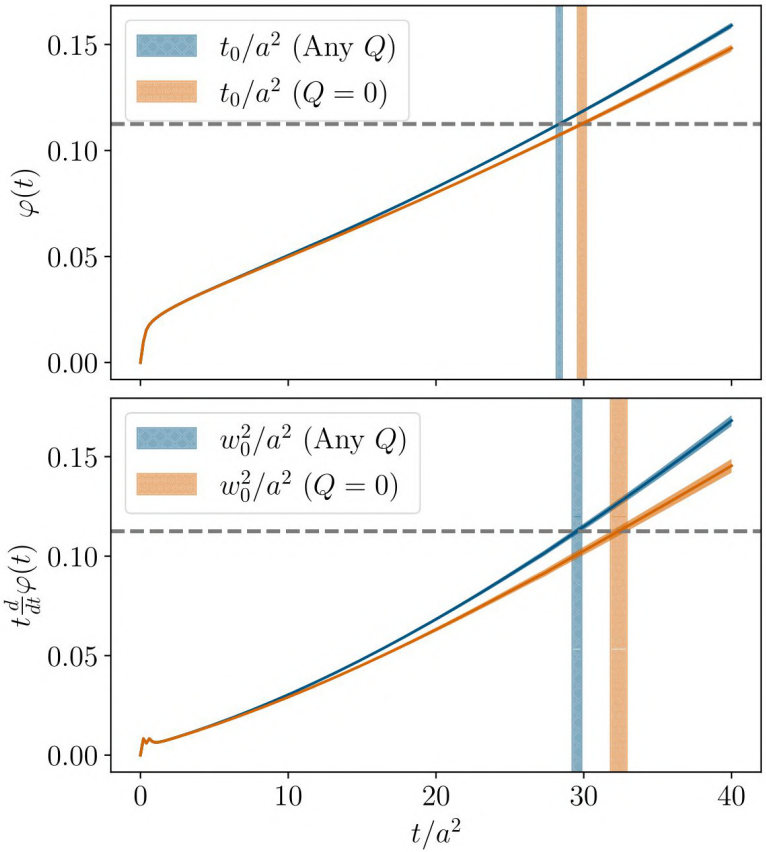

2nd application – SU(N) gradient-flow scales: methods

Numerical setup similar to one used for SU(3) TGF coupling: $L^2 \times L_s^2$ lattices with

- 3 values of $b = \beta/(2N^2)$ (lattice spacings down to ≈0.025 fm) for each $N = 3, 5, 8$
- 2 values of L large enough to neglect finite-L exponentials (checked *a posteriori*) for each (N, b)
- 3-4 values of L_s for each (N, b, L) (aspect ratio not fixed)

2nd application – SU(N) gradient-flow scales: methods

Numerical setup similar to one used for SU(3) TGF coupling: $L^2 \times L_s^2$ lattices with

- 3 values of $b = \beta/(2N^2)$ (lattice spacings down to ≈0.025 fm) for each $N = 3, 5, 8$
- 2 values of L large enough to neglect finite-L exponentials (checked *a posteriori*) for each (N, b)
- 3-4 values of L_s for each (N, b, L) (aspect ratio not fixed)

Fit of non-projected scale $T_0 = t_0/a^2$: exponential in L_s at largest L

$$T_0(N, b, L_s, L_{\max}) = T_0(N, b)\left[1 - \frac{A}{N^2} e^{-M\hat{L}_s}\right] \qquad \hat{L}_s = \frac{L_s}{\sqrt{8T_0(N, b)}}$$

2nd application – SU(N) gradient-flow scales: methods

Numerical setup similar to one used for SU(3) TGF coupling: $L^2 \times L_s^2$ lattices with

- 3 values of $b = \beta/(2N^2)$ (lattice spacings down to ≈0.025 fm) for each $N = 3, 5, 8$
- 2 values of L large enough to neglect finite-L exponentials (checked *a posteriori*) for each (N, b)
- 3-4 values of L_s for each (N, b, L) (aspect ratio not fixed)

Fit of non-projected scale $T_0 = t_0/a^2$: exponential in L_s at largest L

$$T_0(N, b, L_s, L_{\max}) = T_0(N, b)\left[1 - \frac{A}{N^2} e^{-M\hat{L}_s}\right] \qquad \hat{L}_s = \frac{L_s}{\sqrt{8T_0(N, b)}}$$

Fit of $Q = 0$ scale: also includes power-like term in L_s and L

$$T_0^{(0)}(N, b, L_s, L) = T_0^{(0)}(N, b)\left[1 - \frac{A}{N^2} e^{-M\hat{L}_s} + \frac{B}{N^2 \hat{L}_s^2 \hat{L}^2}\right] \qquad \hat{L} = \frac{L}{\sqrt{8T_0^{(0)}(N, b)}}, \quad \hat{L}_s = \frac{L_s}{\sqrt{8T_0^{(0)}(N, b)}}$$

- Finite-volume effects assumed independent of lattice spacing
- Fits performed both N-by-N and globally, also for t_1, w_0^2

2nd application – SU(N) gradient-flow scales: results (arXiv:2511.07355)

N-by-N fits

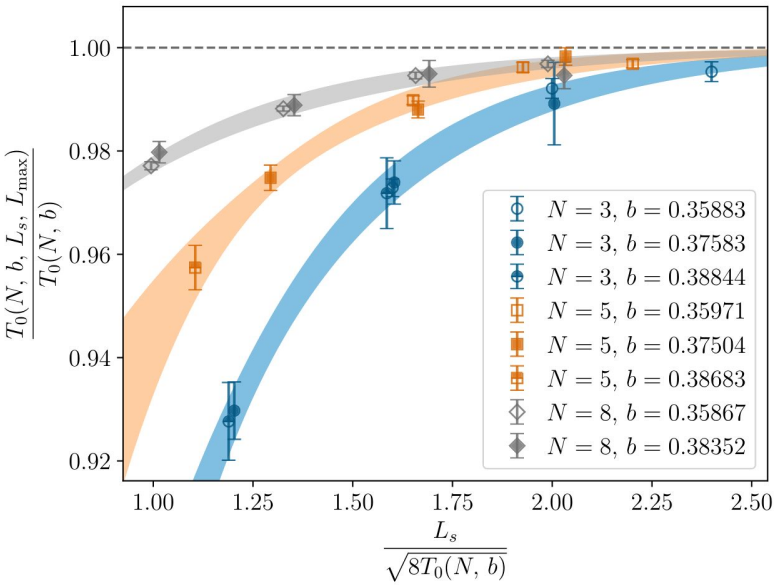

Finite-volume correction on the non-projected scales is exponential and suppressed at large-N

2nd application – SU(N) gradient-flow scales: results (arXiv:2511.07355)

N-by-N fits

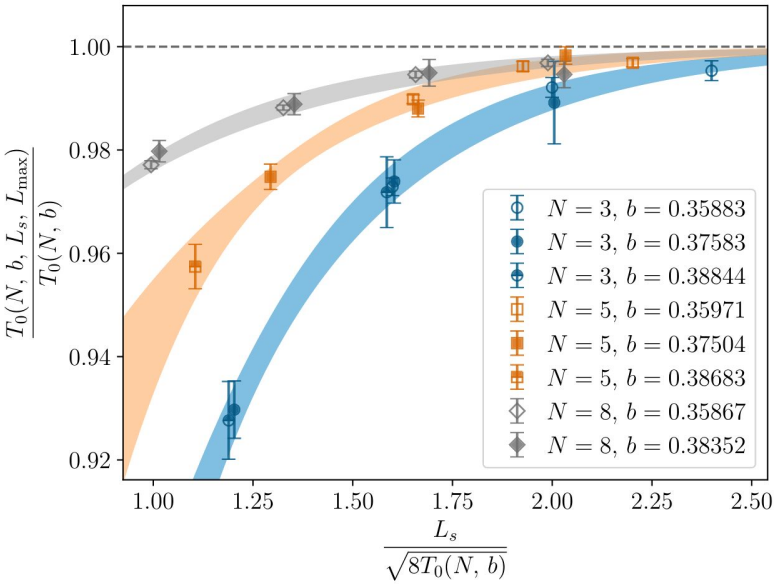

Global fit

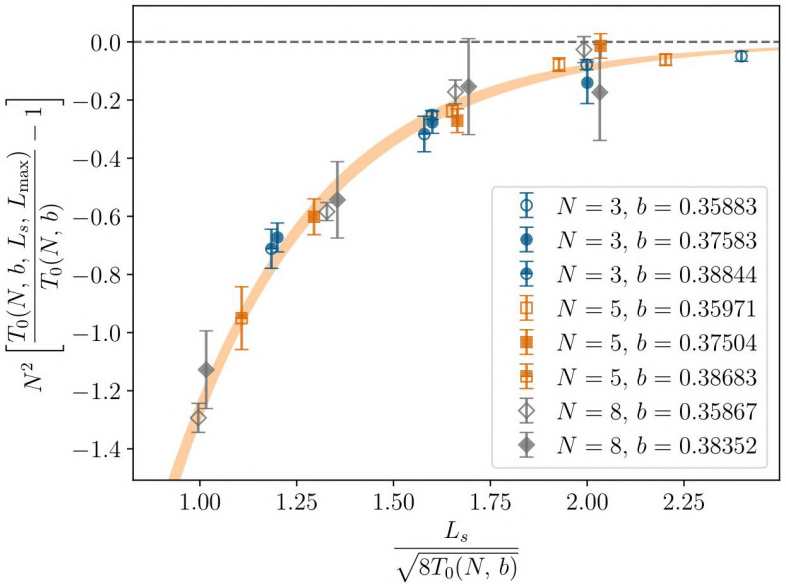

Finite-volume correction on the non-projected scales is exponential and suppressed at large-N

The suppression of the finite-volume correction is $1/N^2$ at leading order as expected

2nd application – SU(N) gradient-flow scales: results (arXiv:2511.07355)

N-by-N fits

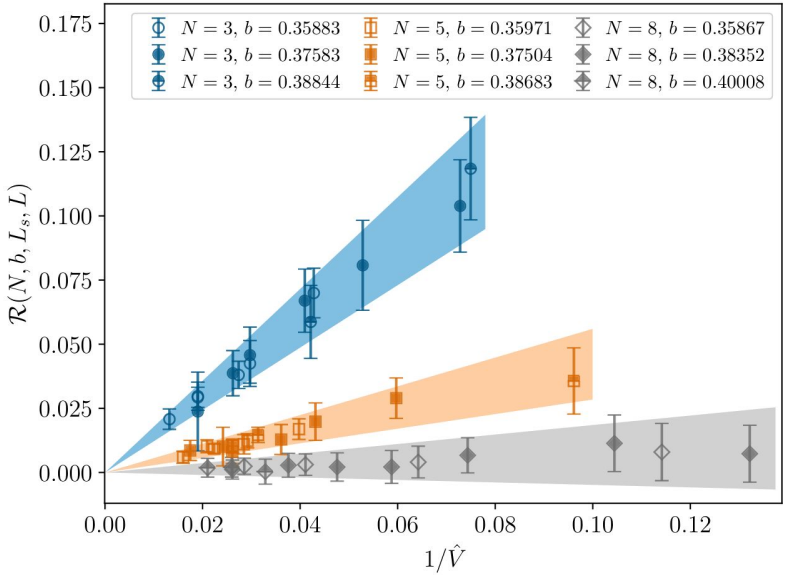

Finite-volume correction on the projected scales has a further $1/V$ contribution

$$\mathcal{R}(N, b, L_s, L) = \frac{T_0^{(0)}(N, b, L_s, L)}{T_0^{(0)}(N, b)} - 1 + \frac{A}{N} e^{-M\hat{L}_s}$$

2nd application – SU(N) gradient-flow scales: results (arXiv:2511.07355)

N-by-N fits

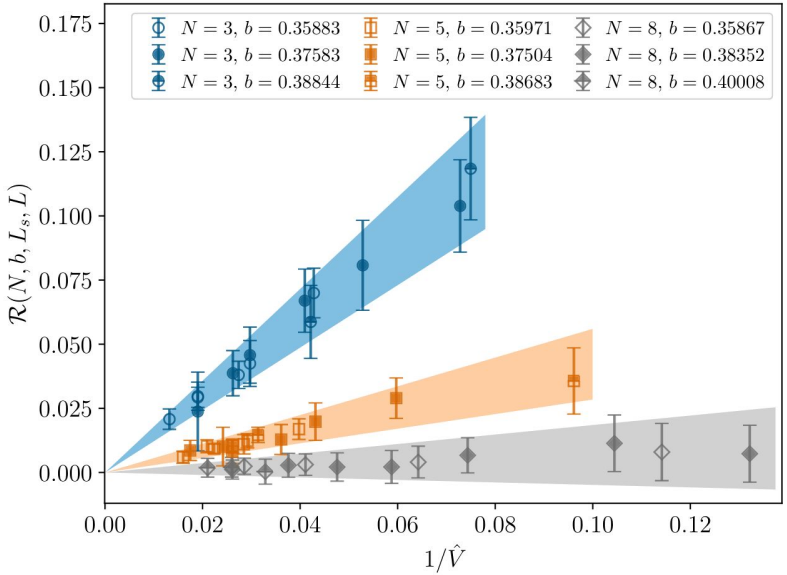

Finite-volume correction on the projected scales has a further $1/V$ contribution

$$\mathcal{R}(N, b, L_s, L) = \frac{T_0^{(0)}(N, b, L_s, L)}{T_0^{(0)}(N, b)} - 1 + \frac{A}{N} e^{-M\hat{L}_s}$$

Global fit

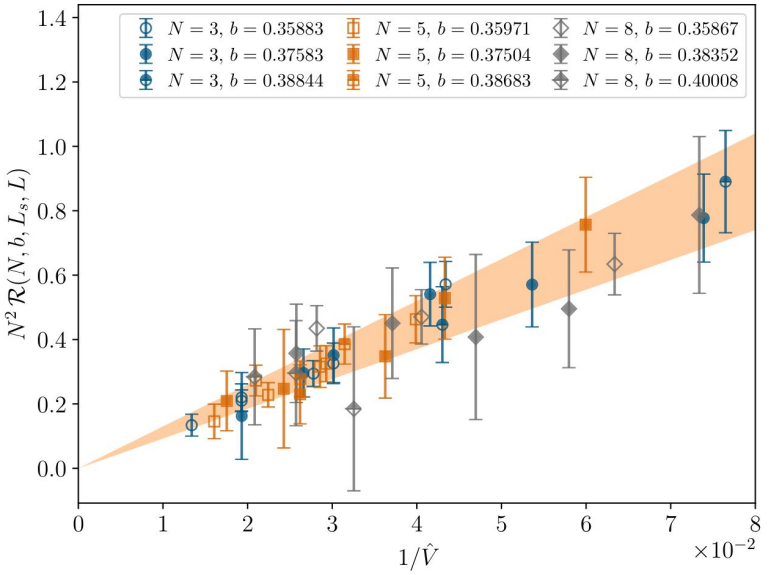

This correction is also suppressed as $1/N^2$ and dominates the exponential contribution, so PTBC gives better control on extrapolation

2nd application – SU(N) gradient-flow scales: results (arXiv:2511.07355)

TBCs significantly reduce finite-volume effects compared to PBCs already at $N = 3$

Determinations with PBCs require $\ell_s \gtrsim 1.6\sqrt{8t_0}$ otherwise center symmetry is broken

TBCs preserve center symmetry down to smaller sizes, enabling meaningful determinations with smaller volumes as $N \to \infty$

Results with TBCs and PBCs converge at large volumes, as expected

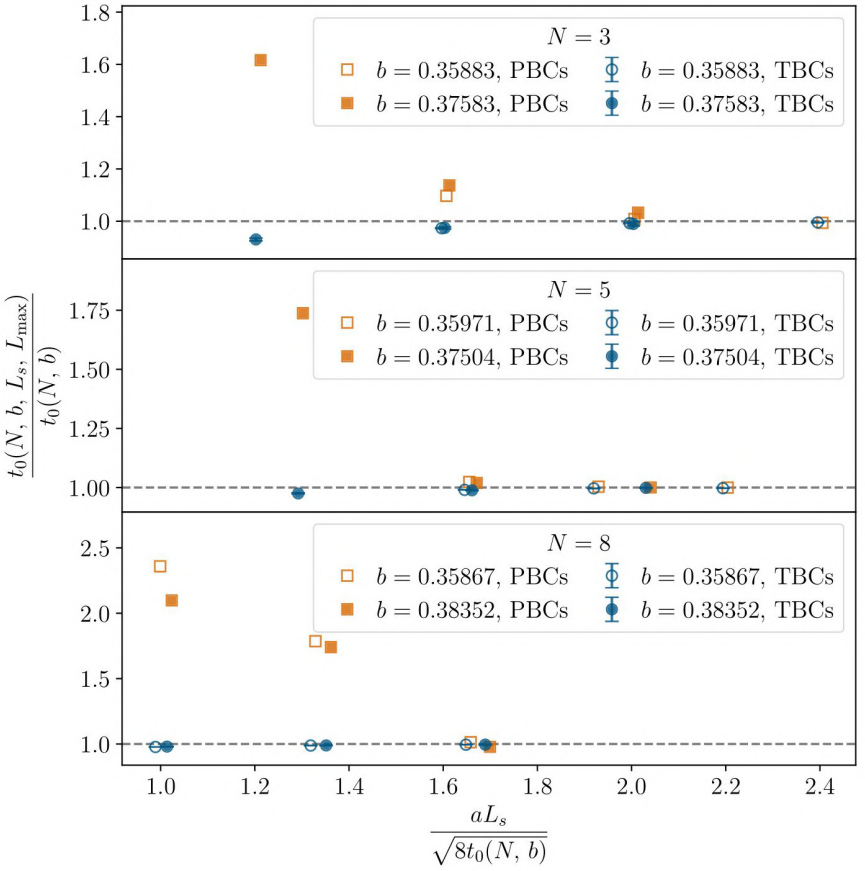

2nd application – SU(N) gradient-flow scales: results (arXiv:2511.07355)

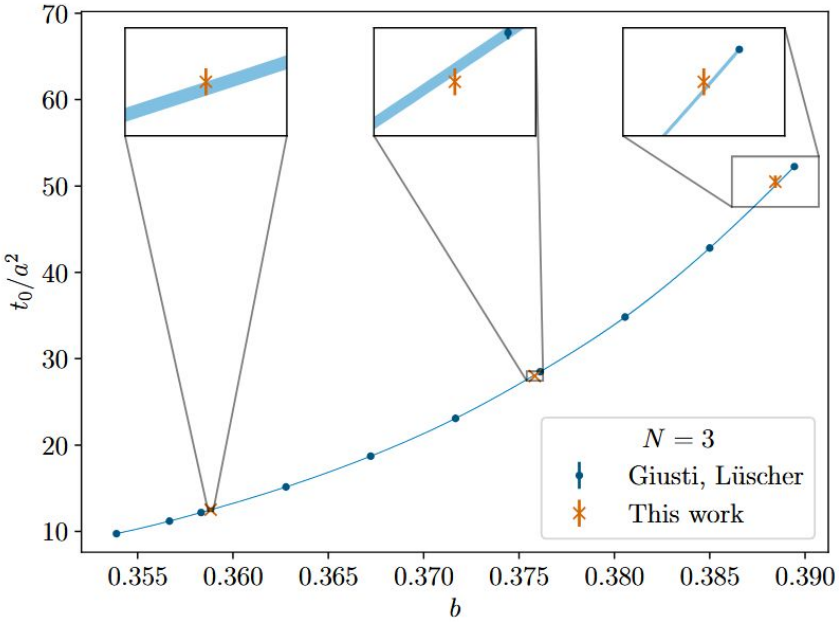

Agreement with literature for $N = 3$
(Giusti and Lüsher, 2019)
and coarsest spacing of $N = 5$
(Cè et al., 2016), other results are new

2nd application – SU(N) gradient-flow scales: results (arXiv:2511.07355)

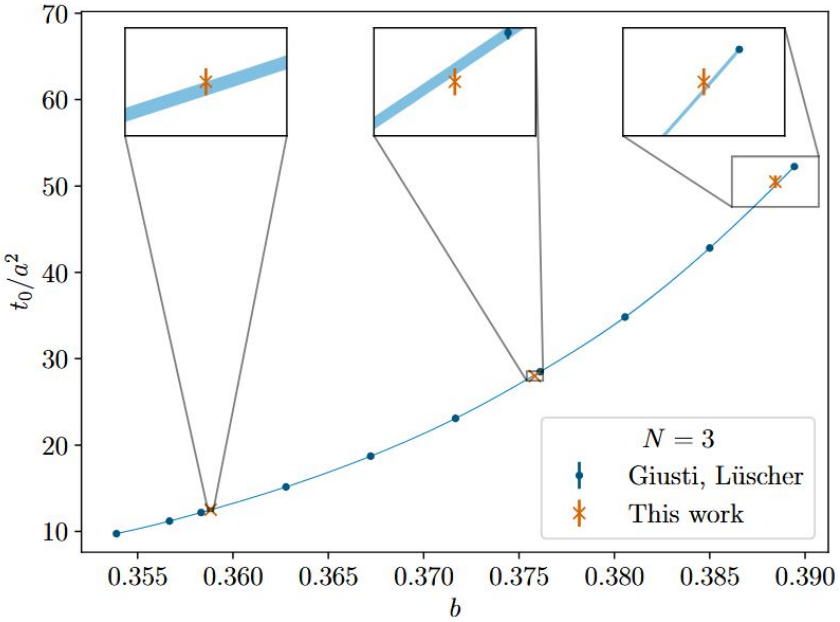

Agreement with literature for $N = 3$ (Giusti and Lüsher, 2019) and coarsest spacing of $N = 5$ (Cè et al., 2016), other results are new

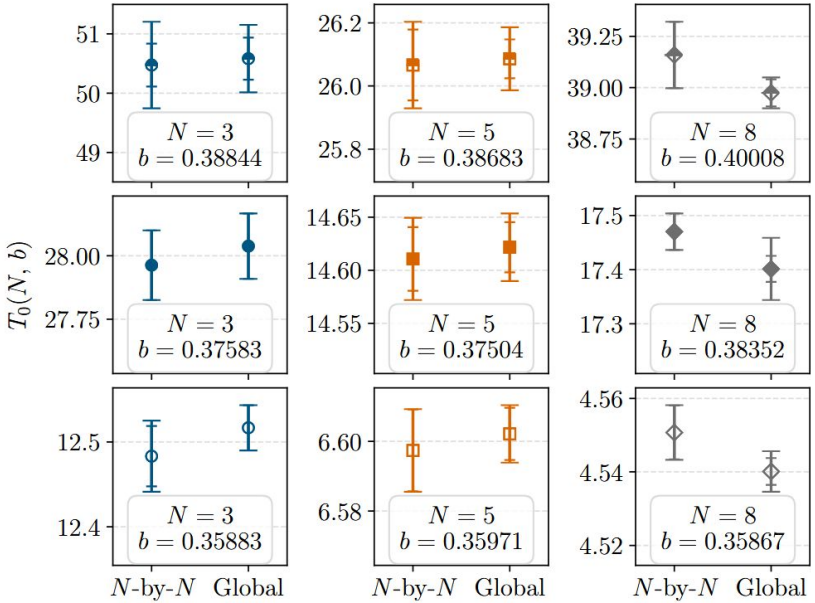

Difference between fits with/without projection used to determine a systematic uncertainty, global and N-by-N analysis agree with sub-percent accuracy

Future application – Multicanonical PTBC: motivation

Topological freezing causes simulations to get stuck in $Q = 0$ due to an *algorithmic* inefficiency

Also possible to have a *physical* suppression of $Q \neq 0$ sectors (small volumes, high-temperatures).
Computation of observables highly dependent on Q becomes expensive: with N_s independent samples

$$\langle Q^2 \rangle \ll 1 \Rightarrow \frac{\delta\chi}{\chi} \simeq \sqrt{\frac{1}{N_s \langle Q^2 \rangle}}$$

If $\langle Q^2 \rangle = 0.1$, $N_s = O(10^4)$ to reach 2% precision. Freezing can also worsen the issue.

Future application – Multicanonical PTBC: motivation

Topological freezing causes simulations to get stuck in $Q = 0$ due to an *algorithmic* inefficiency

Also possible to have a *physical* suppression of $Q \neq 0$ sectors (small volumes, high-temperatures).
Computation of observables highly dependent on Q becomes expensive: with N_s independent samples

$$\langle Q^2 \rangle \ll 1 \Rightarrow \frac{\delta\chi}{\chi} \simeq \sqrt{\frac{1}{N_s \langle Q^2 \rangle}}$$

If $\langle Q^2 \rangle = 0.1$, $N_s = O(10^4)$ to reach 2% precision. Freezing can also worsen the issue.

Multicanonical method: add $V(Q_{\mathrm{M}})$ to the action to enhance fluctuations of Q and reweight averages,
Q_{M} less precise but cheaper to compute definition of Q

Idea: combine PTBC and multicanonical method to address both topological freezing and suppression of Q for high-temperature determinations of χ

Future application – Multicanonical PTBC: implementation

Multicanonical potential V_r can be chosen freely for each replica r:

$$S_r[U] \longrightarrow \tilde{S}_r[U] = S_r[U] + V_r(Q_{\mathrm{M}}[U])$$

Requires an additional Metropolis step on each replica after its local update:
computation of Q_{M} on each replica is the largest overhead added to the standard PTBC

Variation of action under swaps of replicas has new term:

$$\Delta S^{(r,s)}_{\mathrm{swap}} \longrightarrow \Delta S^{(r,s)}_{\mathrm{swap}} + \Delta V^{(r,s)}_{\mathrm{swap}}$$

Cheap to compute having already calculated Q_{M}.

Future application – Multicanonical PTBC: implementation

Multicanonical potential V_r can be chosen freely for each replica r:

$$S_r[U] \longrightarrow \tilde{S}_r[U] = S_r[U] + V_r(Q_{\mathrm{M}}[U])$$

Requires an additional Metropolis step on each replica after its local update:
computation of Q_{M} on each replica is the largest overhead added to the standard PTBC

Variation of action under swaps of replicas has new term:

$$\Delta S^{(r,s)}_{\mathrm{swap}} \longrightarrow \Delta S^{(r,s)}_{\mathrm{swap}} + \Delta V^{(r,s)}_{\mathrm{swap}}$$

Cheap to compute having already calculated Q_{M}.

Ideally, the distribution of Q should be almost flat on every replica. Dynamical tuning of V_r:

- Start from simple $V_r(x)$ based on expected distribution
- Every time $x = Q_{\mathrm{M}}$ is measured during the simulation, $V_r(x) \to V_r(x) + \epsilon$ to suppress it

Method already used in literature with standard algorithms (Jhan et al., 2018),
also tested in full QCD with PTBC (Bonanno et al, 2024)

Future application – Multicanonical PTBC: exploratory tests

Tests for $\mathrm{SU}(3)$ at $\beta = 6.6693$ $(a \simeq 0.035 \text{ fm})$
with $V = N_T \times 40^3$, $N_T = 8, 12, 16$
$(T/T_c \simeq 2.3, 1.6, 1.2)$

Q_{M} defined with $n_{\mathrm{cool}} = 2$ cooling steps
Q defined at $t_Q/a^2 = 4$

Future application – Multicanonical PTBC: exploratory tests

Tests for $\mathrm{SU}(3)$ at $\beta = 6.6693$ $(a \simeq 0.035\ \mathrm{fm})$
with $V = N_T \times 40^3$, $N_T = 8, 12, 16$
$(T/T_c \simeq 2.3, 1.6, 1.2)$

Q_M defined with $n_\mathrm{cool} = 2$ cooling steps
Q defined at $t_Q/a^2 = 4$

No tuning of V_r, simple guess based on DIGA:

$$V_r(Q) = \left(1 - 0.1\frac{r}{N_r - 1}\right)\log(p_Q/p_0)$$

$$p_Q = e^{-\langle Q^2\rangle} I_Q(\langle Q^2\rangle)\,,\ I_n(x) = \sum_{k=0}^{\infty} \frac{(x/2)^{2k+n}}{k!(k+n)!}$$

up to a maximum Q_M and with a first estimate of $\langle Q^2\rangle$

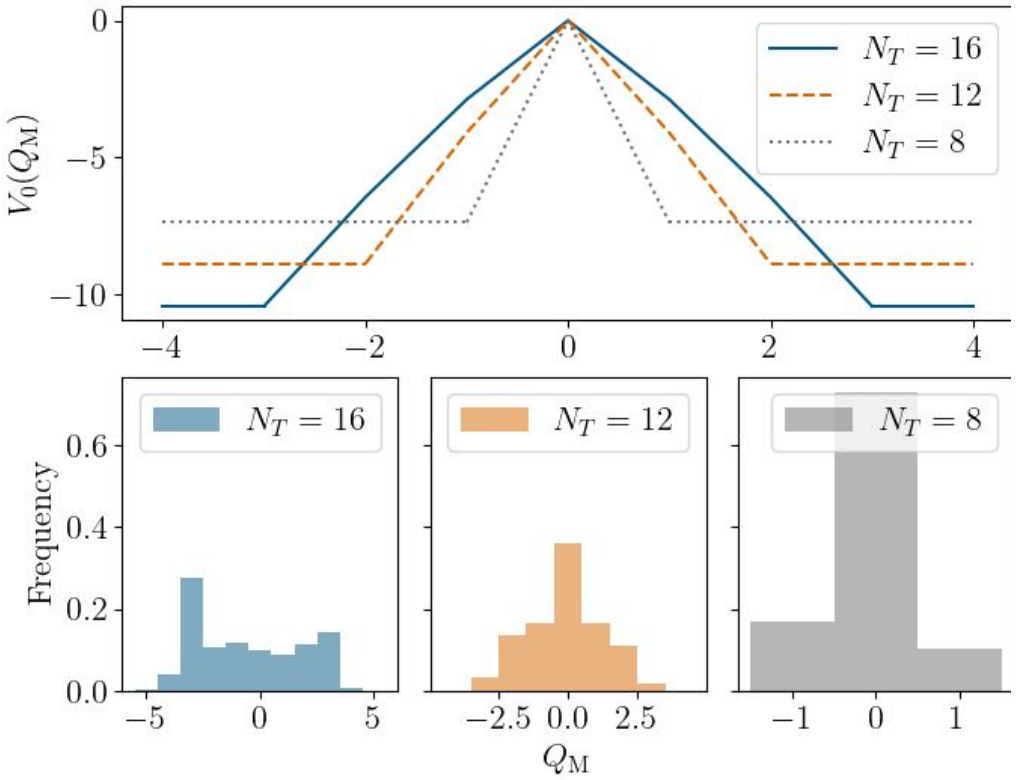

Future application – Multicanonical PTBC: exploratory tests

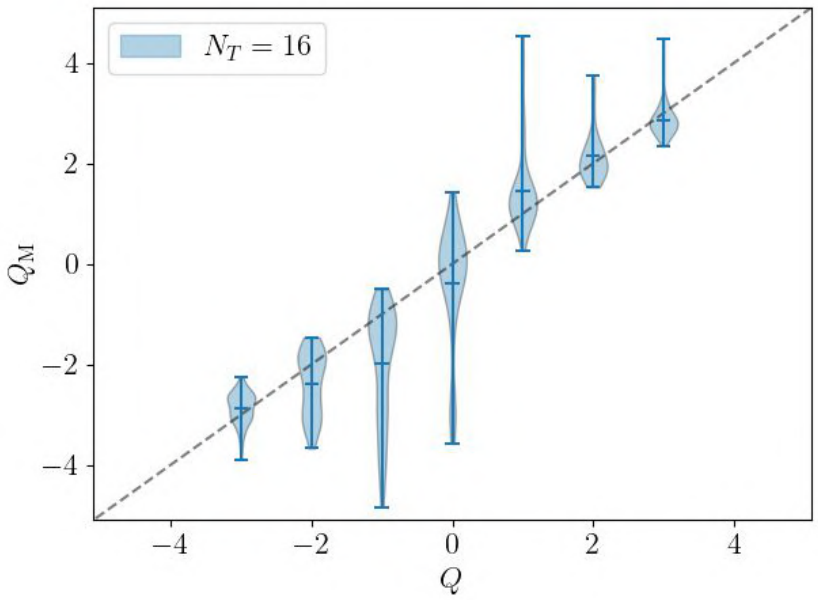

Correlation between Q and Q_{M}:
a few configurations are overly enhanced,
more cooling might improve efficiency

Future application – Multicanonical PTBC: exploratory tests

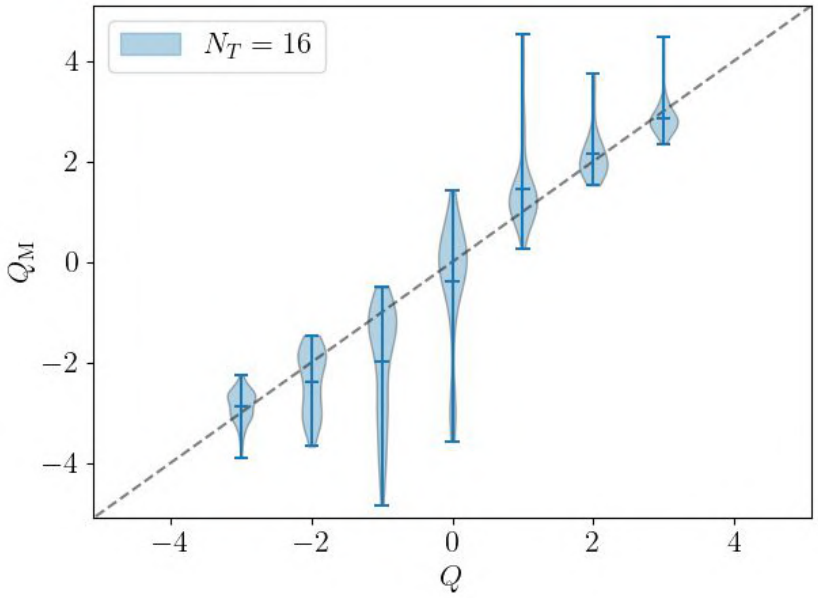

Correlation between Q and Q_M:
a few configurations are overly enhanced,
more cooling might improve efficiency

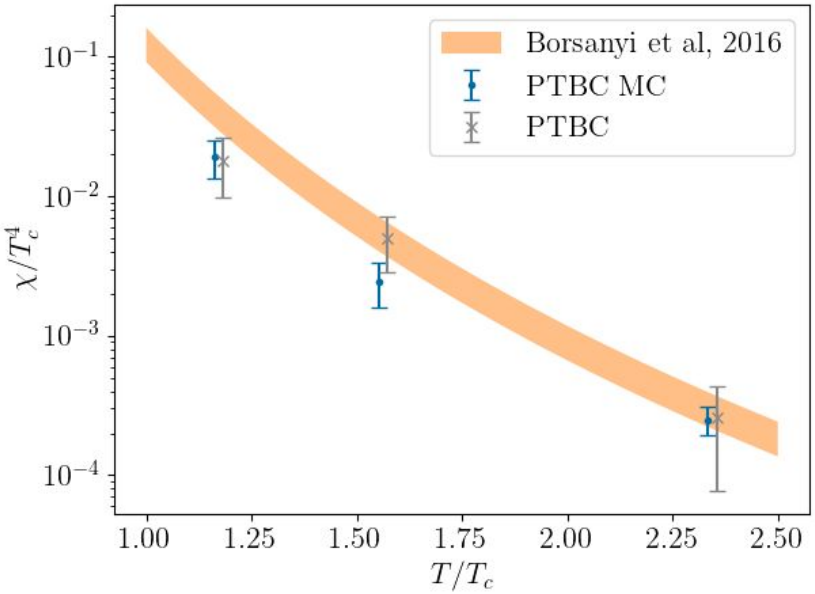

Results for the topological susceptibility at similar computational effort:
gain of MC method clear only at $T \simeq 2.3T_c$

Conclusions – summary of results

Main results

PTBC algorithm is an efficient solution to topological freezing in SU(N) YM theories

- Applied to the SU(3) TGF coupling, allowed to check for biases in the projection to $Q = 0$ used as a workaround to freezing with standard algorithms
- Applied to the SU(N) scale setting, allowed to quantify and avoid $1/V$ finite-volume effects in the gradient-flow scales

Conclusions – summary of results

Main results

PTBC algorithm is an efficient solution to topological freezing in SU(N) YM theories

- Applied to the SU(3) TGF coupling, allowed to check for biases in the projection to $Q = 0$ used as a workaround to freezing with standard algorithms
- Applied to the SU(N) scale setting, allowed to quantify and avoid $1/V$ finite-volume effects in the gradient-flow scales

Future outlooks

- Application of the PTBC algorithm with multicanonical reweighting to the determination of χ at high temperatures
- Complete the determination of the Λ-parameter for $N = 3, 5, 8$ (and large-N) thanks to results of scale setting and step-scaling (under refinement)
- Studies of high-temperature topology in full QCD (PTBC already implemented)
- Study of finite-volume effects in θ-dependence

Backup – PTBC algorithm: tuning

Tuning of PTBC parameters with simple procedure:

1. Start from guess for N_r and $c(r)$
2. Measure $a(r, r+1)$ and its average $\langle a \rangle$
3. Update $\delta(r) = c(r) - c(r+1)$ as

   $$\delta'(r) = \delta(r) + k\frac{a(r, r+1) - \langle a \rangle}{N_r} \qquad (k \simeq 0.5)$$

   to increase/decrease $a(r, r+1)$ below/above $\langle a \rangle$
4. Iterate 2-3 until $a(r, r+1) \simeq \langle a \rangle$
5. Increase/decrease N_r based on target $\langle a \rangle$, interpolate new $c(r)$ and repeat from 2

Tuning runs are cheap: $a(r, r+1) \sim \langle e^{-\Delta S_{\text{swap}}(r, r+1)} \rangle$ does not depend significantly on Q or the volume if $L \gtrsim 4L_d$, tuning time usually negligible compared to actual simulation

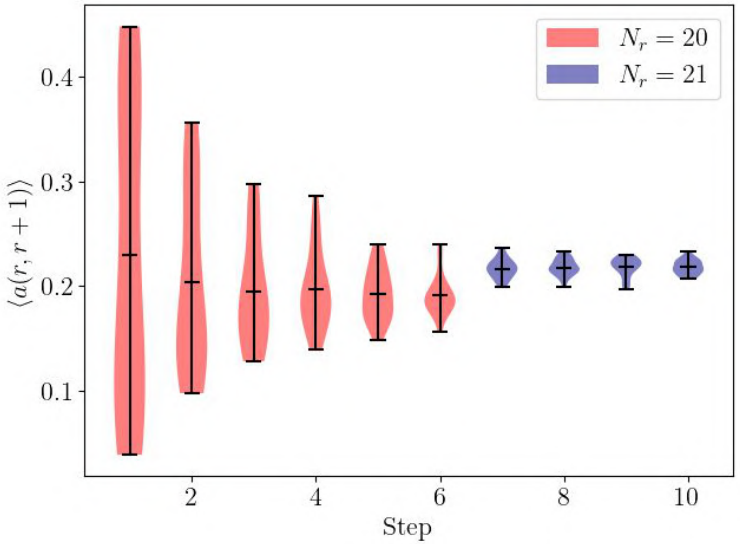

Tuning for $N = 5,\ \beta \simeq 17.9,\ L_d = 3$ starting from simplest guess $c(r) = 1 - r/(N_r - 1)$

Backup – FDIGA predictions for χ and B_2 in TGF scheme

Dilute gas of objects with fractional topological charge $\pm 1/N$ but total must be integer:

$$Z_Q = \mathcal{C} \sum_{n,\overline{n}} \frac{(RV)^{n+\overline{n}}}{n!\overline{n}!} \delta\left(n - \overline{n} - NQ\right) \qquad Z(\theta) = \sum_Q e^{iQ\theta} Z_Q$$

with R probability to create a fractional instanton per unit volume (Gonzalez-Arroyo, 2023 for a review)

Taking derivatives w.r.t. θ for $N = 3$:

$$V\chi(x) = \frac{x}{18}\left(2 - \frac{3(2+x)}{2+e^{3x/2}}\right)$$

$$B_2(x) = \frac{1}{9} + \frac{x(2+x)}{2(2+e^{3x/2})} - \frac{x^2(8+x)}{8 - 8e^{3x/2} + 12x}$$

with $x = RV$. Semi-classical estimation of R unreliable, measured χ can be used instead to obtain a consistency prediction for B_2

Backup – Continuum and large-N limits of scale ratios

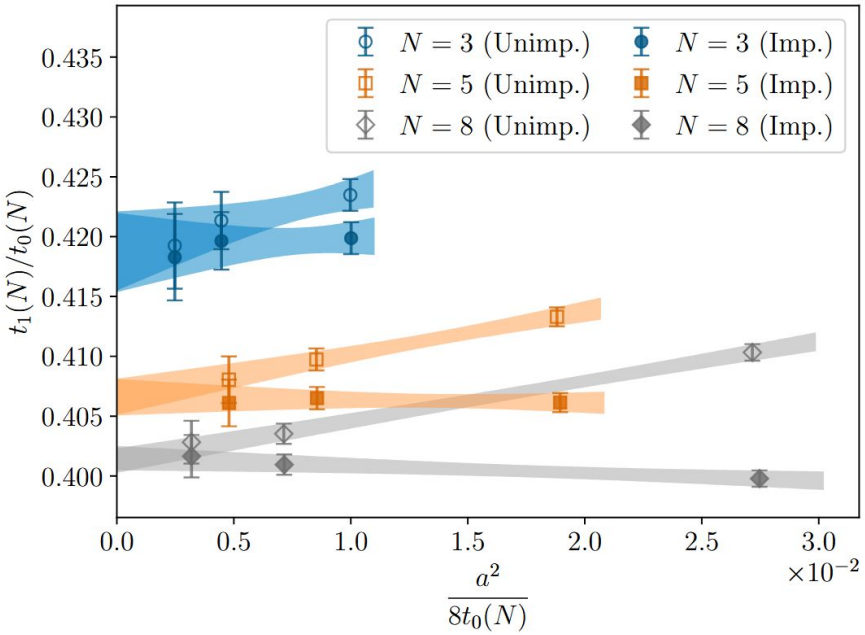

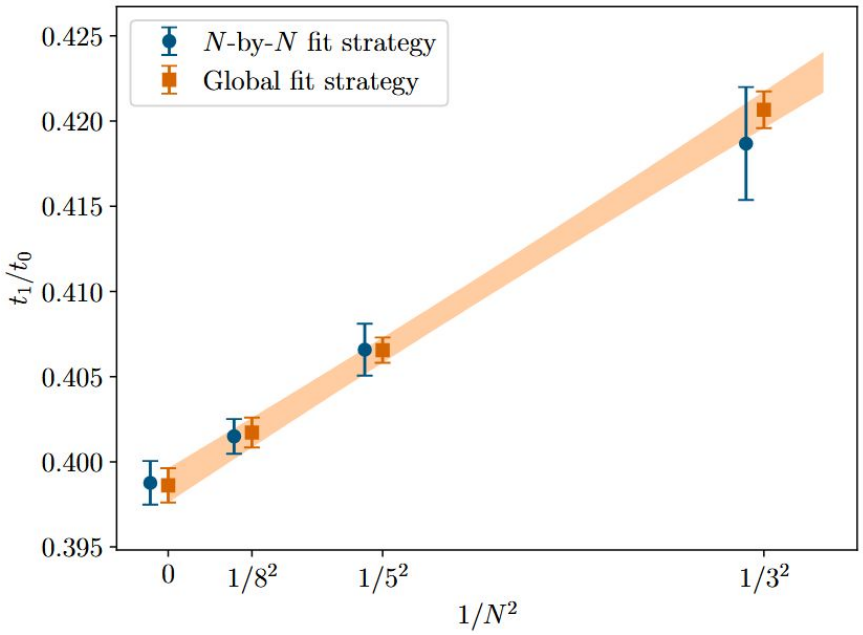

Ratios of scales computed naively assuming independent determinations (statistical errors are overestimated) and extrapolated to the continuum and large-N limits. N-by-N fits and a global fit imposing N-independent lattice artifacts give compatible results